ARTICLE

Physical and Mechanical Properties of *Catalpa bungei* Clones and Estimation of the Properties by Near-Infrared Spectroscopy

Rui Wang, Lanlan Shi and Yurong Wang[*]

Research Institute of Wood Industry, Chinese Academy of Forestry, Beijing, 100091, China

[*]Corresponding Author: Yurong Wang. Email: yurwang@caf.ac.cn

ABSTRACT

Air-dry density, modulus of rupture (MOR), modulus of elasticity (MOE), compressive strength parallel to grain, and hardness of *Catalpa bungei* clones were investigated in this study with feasibility of predicting these properties by near-infrared (NIR) spectroscopy. The best candidate 'Luoqiu 3' has been selected from three clones based on wood physical and mechanical property indices. Lower values of wood physical and mechanical properties have been found in the corewood compared to the outerwood. There were significant positive correlations between the air-dry density and mechanical properties. Information from cross section for air-dry density, compressive strength parallel to grain, and hardness yielded prediction models with better effects, along with the best MOR and MOE modeling effects resulted from average sections' spectra collection. Multiplicative scatter correction (MSC) + Savitzky-Golay (S-G) smoothing method has been proved to be the most applicable way. In addition, the predictions from five-point sampling method were slightly better than three-point one. Overall, results suggest NIR spectroscopy was viable to predict the physical and mechanical properties of *C. bungei* clones with methods developed in this study proved effective in preliminary screening.

KEYWORDS

C. bungei; wood density; mechanical properties; near-infrared spectroscopy

1 Introduction

Catalpa bungei, as a plant of the Catalpa genus of Bignoniaceae with more than 2000-year cultivation history, is a unique and valuable ornamental timber tree, native to China. The wood of *C. bungei* is widely used in high-grade furniture, decoration, shipbuilding, instruments, military industry, and other aspects. With the development of the economy, the growth of population, and the improvement of living standards, people's demand for precious wood species has increased sharply [1]. The above phenomenon has led to a sharp decline in the number of *C. bungei* trees, a huge shortage in timber, and high prices. To solve the contradiction between supply and demand of *C. bungei* wood resources in China, it is necessary to carry out superior clone selection, directional cultivation and strengthen the efficient processing and utilization of wood. Therefore, it is of great practical significance to systematically study the wood properties of *C. bungei* and select out excellent clone. And the clone with the highest physical and mechanical properties will be selected as the optimal clone to meet the material requirements in applications such as construction and furniture.

As a heterogeneous and anisotropic natural polymer material, research on the physical and mechanical properties of wood plays an important role in the rational use of wood and engineering design [2]. To better understand the quality and performance of *C. bungei* wood products, air-dry density (the ratio of its air-dry mass to its volume), modulus of rupture (MOR, a measure of the ultimate resistance of wood when subject to an applied load), modulus of elasticity (MOE, a measure of resistance to distortion that wood undergoes when subject to an applied load), compressive strength parallel to grain (the strength of a specimen under load applied to all the compression surfaces parallel to the direction of the wood fibers), and hardness (the property of being resistant to pressure) are critical [3–5]. The technological properties and other physical and mechanical properties of wood can usually be judged according to the density of wood [6,7].

Academic circles have carried out research on the physical and mechanical properties of *C. bungei* 'Wanqing number 1', *Catalpa bungeana*, and *C. bungei* 'Wanqiu 8401' [8,9]. Liu et al. [8] conducted a study on the *C. bungei* 'Wanqing number 1', and the results showed that the wood had good mechanical properties and was beneficial to industrial production, with the MOR value of 82.3 MPa, MOE value of 10.0 GPa and compressive strength parallel to grain value of 41.5 MPa. In addition, the physical and mechanical properties of *C. bungei* 'Wanqiu 8401' are similar to those of *Catalpa bungeana* which is widely used in production, and *C. bungei* 'Wanqiu 8401' is better for promotion and application than *Catalpa bungeana* because of its higher growth [9]. At present, there are few systematic reports on the wood properties of the newly cultivated Catalpa clones.

Conventional methods for determining wood density, MOR, MOE, compressive strength parallel to grain, and hardness required extensive sample preparation and destructive testing. Near-infrared (NIR) spectroscopy has developed over years as a rapid, reliable, and non-destructive method in wood property assessment [10]. NIR spectroscopy has been used to predict wood air-dry density successfully in many tree species, including *Pinus taeda* [11], *Populus* [12], *Eucalyptus tereticornis* [13], and Mongolian oak [14]. In the same way, mechanical properties can also be obtained quantitatively using the NIR spectroscopy and partial least square (PLS) in many species, such as *Caesalpinia Echinata* [15], Southern pine [16], and Poplar [17].

The method of spectra acquisition differs in two key aspects: one is the spectra acquisition area which can be determined by the sampling points; and the other is the wood section used for model establishment. It could be of high efficacy to collect spectra from radial and tangential section due to dimension of MOR and MOE samples in experiment. Previous studies found that the models based on different sections of bending strength had similar calibration statistics [18,19]. However, a comparison of the prediction of radiate pine with spectra from the radial section *vs.* tangential section suggested the better model prediction on radial section [20]. The pretreatment methods of NIR models applicable for different tree species and properties are different. The first derivative (1stDer) method can eliminate the drift unrelated to the wavelength, and the second derivative (2ndDer) method can eliminate the wavelength linearly related to the wavelength, but the derivative method may degrade the singal-noise ratio (SNR) and expand the role of noise in the spectra [21]. The selection of multiplicative scatter correction (MSC) method can eliminate the difference of scattering information in the spectra [22]. Li et al. [23] established MOR and MOE calibrations of thermally modified southern pine wood with 2ndDer, while Yu et al. [14] found that 1stDer + Savitzky-Golay (S-G) was better than other pretreatment methods for predicting MOR and MOE of Mongolian oak. In general, several studies used NIR spectroscopy to predict MOE and MOR, but the prediction for compressive strength parallel to grain and hardness was not fully explored.

To our knowledge, little effort has been devoted to investigate the physical and mechanical properties of the newly bred 3 *C. bungei* clones, 'Luoqiu 2', 'Luoqiu 3', and 'Luoqiu 5', along with no literature found regarding the applicability of NIR spectroscopy in predicting catalpa wood properties. Therefore, the specific objectives were: (1) to assess the air-dry density, MOR, MOE, compressive strength parallel to grain, and

hardness by conventional methods and select the optimal clone from 3 *C. bungei clones*; (2) to investigate the correlation between physical and mechanical properties of *C. bungei* clones; (3) to evaluate the feasibility of NIR spectroscopy to determine physical and mechanical properties of *C. bungei* clones and explore the best modeling methods for each performance.

2 Materials and Methods

2.1 Materials

The sample trees of *C. bungei* clones have been planted at a forest farm in Tianshui City, Gansu Province (34°06′–34°48′ north latitude, 105°25′–106°43′ east longitude), China. The mean annual precipitation for the site was 600 mm. We studied three 13-year-old *C. bungei* clones, 'Luoqiu 2', 'Luoqiu 3', and 'Luoqiu 5'. Among them, 'Luoqiu 2' and 'Luoqiu 5' are half-sib families. The 13-year-old *C. bungei* woods consist of juvenile and mature woods. The basic information of experimental materials was shown in Table 1. A total of 10 trees were used as samples for wood property testing, and the wood segment between 1.5 to 3.5 m in height of each tree was intercepted for performance index determination.

Table 1: Basic information of experimental materials

Name of clones	Number (n)	Height (m)	Diameter at breast height (cm)
Luoqiu 2	3	11.9 ± 1.6	16.9 ± 1.9
Luoqiu 3	4	11.8 ± 0.6	16.4 ± 1.8
Luoqiu 5	3	11.9 ± 0.1	15.7 ± 1.2

2.2 Specimen Preparation

As shown in Fig. 1, all the logs were cut into 350–450 mm-long segments. 400 and 450 mm-long wood segments were used to make blank strips with a cross-section of 30×30 mm. The blank strips near the pith distributed in growth rings 3–6 (corewood) were numbered H1–H2 and the blank strips close to the bark distributed in growth rings 7–12 (outerwood) were numbered S1–S4. Sample number and dimensions were listed in Table 2. Blank strips with a cross-section size of 70 mm $\times$ 70 mm were continuously prepared from 350 mm long wood segments, wherein S1 and S2 sampling positions were between the pith and the bark. 24 hardness samples were prepared from each clone, up to 72 in total.
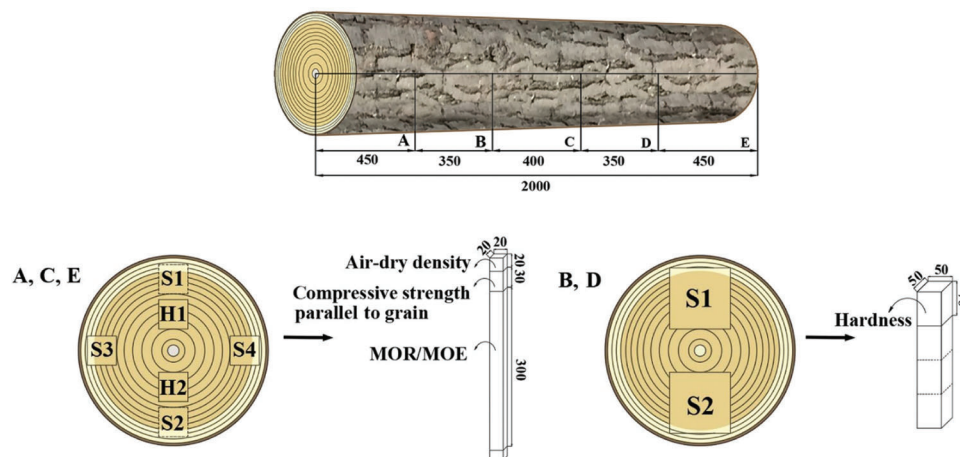

Figure 1: The procedure of preparing the wood samples (mm) for measuring the air-dry density, compressive strength parallel to grain, MOR/MOE, and hardness

Table 2: Number and dimensions for physical and mechanical properties testing

Properties	Number (n)				Dimensions (T × R × L) (mm × mm × mm)
	Luoqiu 2	Luoqiu 3	Luoqiu 5	Total number	
Air-dry density	29	38	29	96	20 × 20 × 20
MOR/MOE	35	46	37	118	20 × 20 × 300
Compressive strength parallel to grain	30	41	31	102	20 × 20 × 30
Hardness	24	24	24	72	50 × 50 × 70

2.3 Measurement of Air-Dry Density and Mechanical Properties

Specimens for the physical and mechanical test were cut into standard dimensions and conditioned at 20°C and 65%RH. All defects such as wood cracks, knot, and reaction wood were eliminated and the directions of the samples were determined. The samples were then conditioned to an equilibrium moisture content of approximately 12%. The determination of the air-dry density was based on national standard GB/T 1933-2009 "*Method for determination of the density of wood*" [24]. MOE, MOR, compressive strength parallel to grain, and hardness were determined by using a universal test machine Instron 5580 (Instron, Norwood, MA, USA), according to the GB/T 1936-2009 "*Method of determination of elasticity in static bending of wood*" [25], GB/T 1936-2009 "*Method of testing in bending strength of wood*" [26], GB/T 1935-2009 "*Method of testing in compressive strength parallel to grain of wood*" [27], and GB/T 1941-2009 "*Method of testing in hardness of wood*" [28].

2.4 NIR Spectra Acquisition

NIR spectra with wavelength ranging from 350–2500 nm were acquired in a spectrometer (ASD, North Sutton, NG, USA) in the diffuse reflectance mode. Two bifurcated fiber optic probes were used to obtain spectral information directly from 10 mm above the sample surface with a spot diameter of approximately 15 mm. To overcome sample moisture content fluctuations, all measurements were taken in a controlled environment with settings at 40%–50% relative humidity and air temperature of 20°C by adjusting the air conditioning and humidifier. For each specimen, 30 scans were acquired and averaged to yield a single NIR spectrum. The NIR spectra of air-dry density samples were collected from cross sections (Fig. 2a). NIR spectra were captured from cross sections, radial sections and tangential sections of compressive strength parallel to grain (Fig. 2b) and hardness (Fig. 2c), while those of MOR/MOE were collected from both the radial and tangential sections (Fig. 2d). The spectra from point 1, point 3, and point 5 were collected when the three-point sampling method was selected.
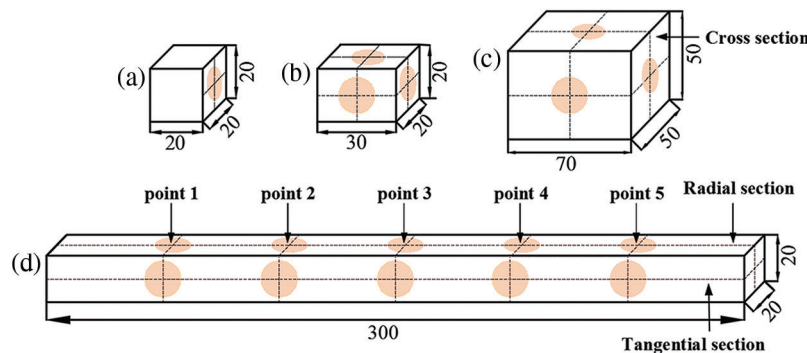

Figure 2: Spectra sampling position for physical and mechanical properties samples: air-dry density (a); compressive strength parallel to grain (b); hardness (c); MOR/MOE (d)

2.5 Multivariate Data Analysis

PLS method has become one of the common methods of model quantitative correction in the wood science field [29]. The relationship of actual value and spectral data for physical and mechanical properties was developed by PLS regression analysis with full cross-validation using the Unscrambler 9.7 software. To obtain better prediction effects, model development was based on wavelengths ranging from 400–2500 nm.

Given undesirable factors affecting the quality of NIR spectra, including spectral information independent of modeling properties, baseline correction, and background noise, it is vital to apply pretreatment methods ahead of PLS, such as 1stDer, 2ndDer, MSC, and S-G smoothing method. Several statistical measures were also used to compare the PLS models, such as the coefficient of determination of calibration (Rc^2), the coefficient of determination of prediction (Rp^2), the standard error of calibration (SEC), the standard error of prediction (SEP) and the ratio of performance to deviation (RPD).

3 Results and Discussion

3.1 Determination of the Physical Properties of C. bungei Clones

3.1.1 Air-Dry Density

Table 3 showed the specific statistics of the air-dry density of 3 *C. bungei* clones. The mean value of the air-dry density of the 3 clones ranged from 0.492 to 0.537 g·cm^{-3}. The results of variance analysis for the density of the 3 *C. bungei* clones showed that the effects of different clones on the air-dry density were significantly different (*P*-value<0.05). Through the comparison among different clones, it was concluded that the air-dry density value of 'Luoqiu 3' showing the highest value at 0.537 g·cm^{-3}, followed by 'Luoqiu 2' and 'Luoqiu 5'. Compared with other catalpa clones, 21-year-old *C. bungei* 'Wanqiu 8401' with air-dry density value of 0.502 g·cm^{-3}, 'Luoqiu 2' and 'Luoqiu 3' had higher air-dry density values [9].

Table 3: The statistics for air-dry density, MOR, MOE, compressive strength parallel to grain, and hardness

	Name of clones	Air-dry density (g·cm^{-3})	MOR (MPa)	MOE (GPa)	Compression strength (MPa)	Hardness (N)			
						Cross section	Radial section	Tangential section	3 sections
Average	Luoqiu 2	0.524b	89.1b	10.8b	59.6b	3822b	3005b	3039a	3259b
	Luoqiu 3	0.537a	94.2a	12.0a	62.0a	4474a	3327a	3008a	3603a
	Luoqiu 5	0.492c	82.2c	10.7b	56.5c	3458c	2596c	2358b	2804c
	3 clones	0.519	88.9	11.3	59.6	3848	2927	2763	3168
Standard deviation	Luoqiu 2	0.0171	10.7	0.895	3.30	460	250	342	300
	Luoqiu 3	0.0256	11.1	0.954	4.45	290	286	411	228
	Luoqiu 5	0.0272	9.80	1.01	4.66	261	278	211	203
	3 clones	0.0305	11.7	1.15	4.85	532	399	455	406
Variable coefficient (%)	Luoqiu 2	3.46	12.0	8.27	5.42	12.1	8.32	11.3	9.20
	Luoqiu 3	4.78	11.8	7.92	7.18	6.49	8.60	13.7	6.34
	Luoqiu 5	5.54	12.0	9.47	8.26	7.55	10.7	8.95	7.23
	3 clones	5.88	13.1	10.2	8.13	13.8	13.6	16.5	12.8

Note: The results of multiple comparisons are indicated by the letters a, b and c in the table, where *P* < 0.05.

3.1.2 Radial Variation of Air-Dry Density

Radial variation of physical and mechanical properties is conducive to the improvement and rational utilization of *C. bungei* wood. Fig. 3a indicated that the air-dry density exhibited a trend of gradually increasing from near the pith to near the bark. From the corewood to the outerwood, the air-dry density of 'Luoqiu 2', 'Luoqiu 3', and 'Luoqiu 5' wood increased by 3.25%, 3.77%, and 7.79%, respectively. There were significant differences in air-dry density between two parts of 3 clones. For the three *C. bungei* clones, there are few studies on radial variation so far. The radial variation of catalpa was in accordance with that of Chinese fir and *Populus deltoides* CL. '55/65' [17,30].
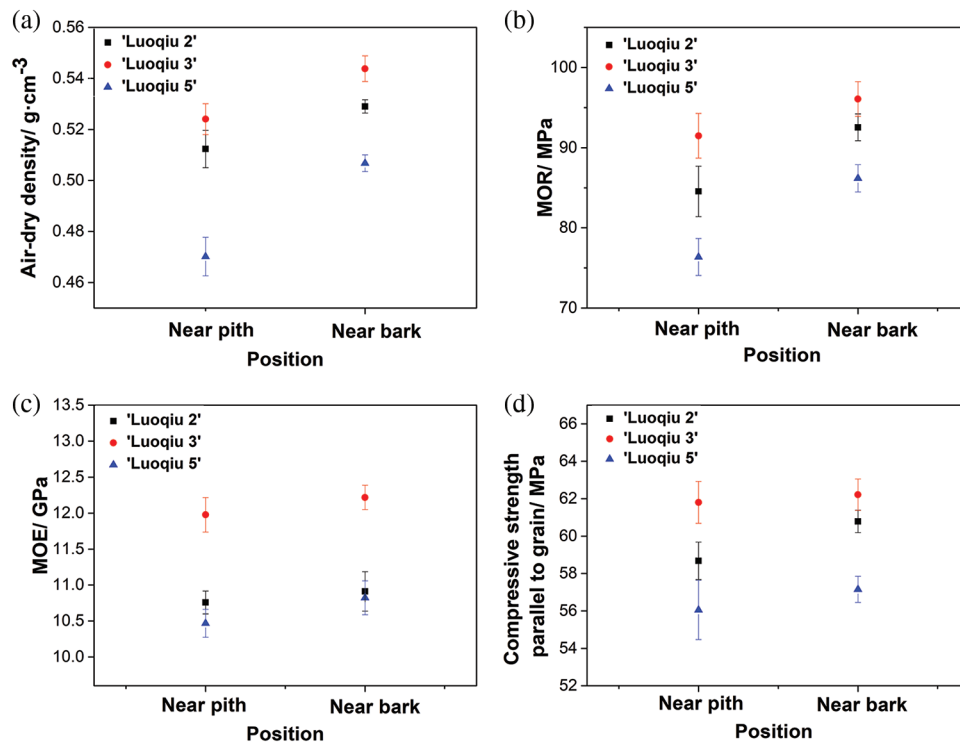

Figure 3: Radial variation of physical and mechanical properties of 3 *C. bungei* clones: air-dry density (a); MOR (b); MOE (c); compressive strength parallel to the grain (d)

3.2 Determination of the Mechanical Properties of C. bungei Clones

3.2.1 Modulus of Rupture

The statistical results of main mechanical properties for different *C. bungei* clones were shown in Table 3. The MOR ranged from 82.2 to 94.2 MPa. 3 *C. bungei* clones, in descending order of MOR were: 'Luoqiu 3' (94.2 MPa), 'Luoqiu 2' (89.1 MPa), and 'Luoqiu 5' (82.2 MPa). And there were significant differences in MOR among different clones. The average value of the MOR of 3 clones was 88.9 MPa, which was a medium level according to "timber property classification provisions" [31]. Compared with 'Luoqiu 3', 21-year-old *C. bungei* 'Wanqiu 8401' had larger MOR of 114 MPa [9], while 21-year-old *C. bungei* 'Wanqiu 8402' had smaller MOE of 85.8 MPa [9].

3.2.2 Modulus of Elasticity

According to Table 3, the MOE was within the range from 10.7 to 12.0 GPa. 3 *C. bungei* clones, in descending order of MOE, were: 'Luoqiu 3' (12.0 GPa), 'Luoqiu 2' (10.8 GPa), and 'Luoqiu 5' (10.7 GPa). Multiple analysis results showed that at the level of 0.05, there was no significant difference

between 'Luoqiu 2' and 'Luoqiu 5', while there was a significant difference between 'Luoqiu 3' and the other two clones. Compared with 21-year-old *C. bungei* 'Wanqiu 8401', all 3 clones had higher MOE values [9].

3.2.3 Compressive Strength Parallel to Grain

The range of the compressive strength parallel to grain was from 56.5 to 62.0 MPa (Table 3). Compared to different *C. bungei* clones, the compressive strength parallel to grain of 'Luoqiu 3' was the highest, while that of 'Luoqiu 5' was the lowest. The average value of the 3 clones was 59.6 MPa, which reached the high level of my country's standard [31], and was higher than the average value of the compressive strength parallel to grain of hardwood trees in my country (45.0 MPa). Compared with 21-year-old *C. bungei* 'Wanqiu 8401', these three clones had higher compressive strength parallel to grain values [9].

3.2.4 Hardness

As shown in Table 3, the mean values of hardness of 3 sections were 2804, 3259, and 3603 N for 'Luoqiu 5', 'Luoqiu 2', and 'Luoqiu 3', respectively. The cross section had hardness value of 3848 N followed by radial section hardness with 2927 N and tangential section hardness at 2763 N. These results were in good agreement with 3-year-old *C. bungei* C.A.Mey [32]. There were significant differences in cross section hardness, radial section hardness, and average hardness among different clones. Compared with 'Luoqiu 3', 21-year-old *C. bungei* 'Wanqiu 8401' had a lower cross section of 3396 N, a lower radial section hardness of 2933 N, and a higher tangential section hardness of 3139 N.

According to the analysis above, the 13-year-old *C. bungei* wood showed high-grade compressive strength parallel to grain, medium-grade MOR, and low-grade MOE and hardness. Among three catalpa clones, 'Luoqiu 3' exhibited the largest four mechanical properties, in contrast to 'Luoqiu 2' with smallest values. 'Luoqiu 3' as the optimal clone could be suggested for the manufacturing of small-diameter precious wood furniture products because of its satisfied specifications based on solid wood furniture material performance [33]. Based on both physics and mechanics characteristics, 'Luoqiu 3' was selected as the optimal clone from 3 clones.

Compared to 21-year-old *C. bungei* 'Wanqiu 8401', 'Luoqiu 3' had higher air-dry density, compressive strength parallel to grain, MOE, cross section hardness, and radial section hardness. Furthermore, the compressive strength parallel to grain, MOR, and MOE of the 13-year-old 'Luoqiu 3' were superior to those of the 74-year-old natural *C. bungei* C.A.Mey harvested in Lianyungang City, Jiangsu Province, China [34]. It would indicate that the younger 'Luoqiu 3' with higher mechanical properties is more applicable for further popularization and utilization than *C. bungei* 'Wanqiu 8401'.

3.2.5 Radial Variation of Mechanical Properties

Figs. 3b–3d showed the variation trend of the MOR, MOE, and compressive strength parallel to grain of 3 *C. bungei* clones from near the pith to near the bark. In line with the change rule of air-dry density, MOR, MOE, and compressive strength parallel to grain from near the pith were all less than the corresponding mechanical properties from near the bark. The MOR, MOE, and compressive strength parallel to grain of 'Luoqiu 2' outerwood were 9.46%, 1.21%, and 3.60% higher than those of corewood, respectively. Similarly, the three mechanical properties of 'Luoqiu 3' outerwood were 5.00%, 2.00%, and 0.68% higher than those of corewood, respectively. The three mechanical properties of 'Luoqiu 5' outerwood were 16.02%, 3.34%, and 1.96% higher than those of corewood, respectively. In addition, there was no obvious difference between corewood and outerwood of the 3 clones in terms of the MOE and compressive strength parallel to grain. Except for 'Luoqiu 3', the MOR near the pith of 'Luoqiu 2' and 'Luoqiu 5' were significantly different from those near the bark. The variation of outerwood and corewood among kinds of tree species was very different. The MOR, MOE, and compressive strength parallel to grain of outerwood of *Quercus cerris* and Chinese fir were higher than those of corewood [30,35], while *Acacia melanoxylon* showed the opposite

trend of variation [36]. Exploring the differences of mechanical properties of different parts of wood is of great significance to the processing and utilization of wood.

3.3 Correlation among Wood Features

The correlation analysis results of air-dry density and main mechanical properties of 3 *C. bungei* clones were shown in Table 4. Air-dry density showed a high correlation to the four mechanical properties with the correlation coefficient between 0.924 and 0.985, which was consistent with related research conclusions on *Robinia pseudoacacia* wood in artificial forests [37]. The maximum correlation coefficient between wood density and MOE was 0.985, and the lowest correlation coefficient between wood density and hardness was 0.924, indicating that air-dry density had different effects on mechanical properties. The regression analysis of the air-dry density and mechanical properties of *C. bungei* C.A.Mey wood showed that the R^2 value of the correlation fitting degree was between 0.57 and 0.99 [34]. Therefore, the mechanical properties of *C. bungei* wood can be estimated according to its density, which is of economic and scientific significance.

Table 4: Pearson's correlation between wood air-dry density and mechanical properties

	Air-dry density	MOR	MOE	Compressive strength parallel to grain	Hardness
Air-dry density	1	0.978**	0.985**	0.977**	0.924**
MOR		1	0.992**	0.951**	0.936**
MOE			1	0.961**	0.949**
Compressive strength parallel to grain				1	0.976**
Hardness					1

Note: ** represent significant correlation at $P < 0.01$.

The correlation coefficient between different mechanical properties was between 0.936 and 0.992. Among the mechanical indexes, all the correlations were strong and positive in this study, which corresponded with correlation of reported for southern type poplar clones [38]. Among different mechanical properties, the correlation between MOR and MOE was the highest, reaching 0.992, and the correlation between MOR and hardness was the lowest, with a correlation coefficient of 0.936. Similarly, the MOR of 74-year-old *C. bungei* C.A.Mey is positively related to the MOE, and the coefficient of determination reaches 0.804 [34]. It would be beneficial from the significant correlation between the mechanical properties of *C. bungei* to obtain other mechanical properties fast and nondestructively by one mechanical property.

3.4 Raw NIR Spectra of the Specimens

Fig. 4a showed the NIR spectra of 3 *C. bungei* clones. The Catalpa tree samples had strong absorption peaks near 1208, 1461, 1923, 2099, and 2270 nm. The intensity of the lignin band at 1208 (second overtone C-H stretch) was hardness dependent, and similar dynamics were observed at 1461 nm (first overtone O-H stretch), 2099 nm (O-H deform + O-H stretch). NIR spectroscopy mainly reflects the information of each hydrogen-containing group, the absorption peak, and absorption intensity of different groups [39]. Due to the different composition, structure, and content of hydrogen-containing groups in different wood samples, the spectral characteristics will change accordingly [40].
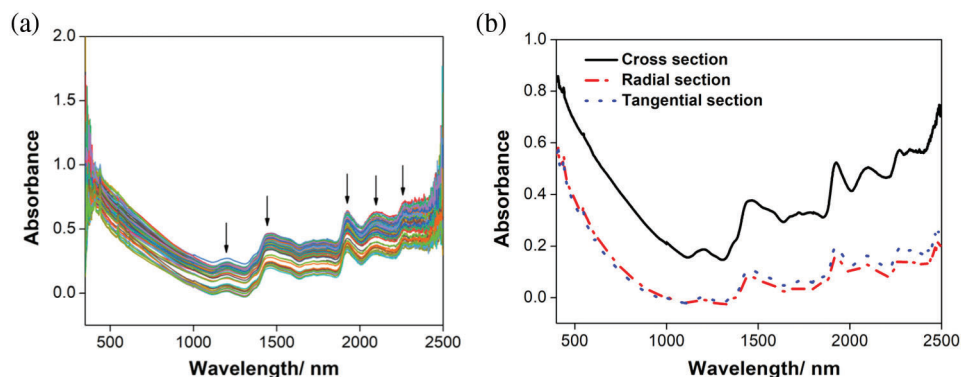
Figure 4: Original NIR spectra of 3 *C. bungei* clones and different sections

The spectra of cross section, radial section, and tangential section of *C. bungei* wood samples were collected, respectively, as shown in Fig. 4b. It can be seen from the figure that the NIR spectra of three sections have certain differences. The spectral absorption intensity of the cross section was significantly greater than the other two sections, which was closely related to the structural characteristics of wood. On the cross section, the information of corewood and outerwood, cell wall thickness, rays, axial parenchyma, and percentage of late wood has been observed. The radial section is a longitudinal section through the main axis of the trunk, where parallel growth rings can be seen and the tangential section is a longitudinal section perpendicular to the rays and parallel to the main axis of the trunk. Therefore, the NIR spectral information obtained from the cross section was richer than that from the radial section and tangential section.

3.5 NIR Model Development of Physical Property

3.5.1 PLS Models of Air-Dry Density

Previous studies have shown that the prediction model based on the spectra collected from the cross section of wood density samples was the best [17,41]. In this study, PLS models were established using the data of the air-dry density measured by the traditional method and the NIR spectra collected from the cross section of the corresponding samples.

Appropriate pretreatment was found to improve the effect of NIR model [42,43]. Therefore, three different pretreatment methods on the prediction efficiency of air-dry density have been applied. There were significant differences among the spectral pretreatment methods (Table 5). It was found that the air-dry density model pretreated by the MSC + S-G smoothing method had the best effect. When using MSC + S-G smoothing method, the Rc^2 value for calibration was 0.861, SEP value was 0.015, and RDP value was 2.07. Fig. 5a showed a good relationship between measured and predicted values by NIR spectra. Based on the results above, NIR spectroscopy technology can be used to predict the air-dry density of *C. bungei*.

Table 5: Comparison of the results of different pretreatment methods for air-dry density

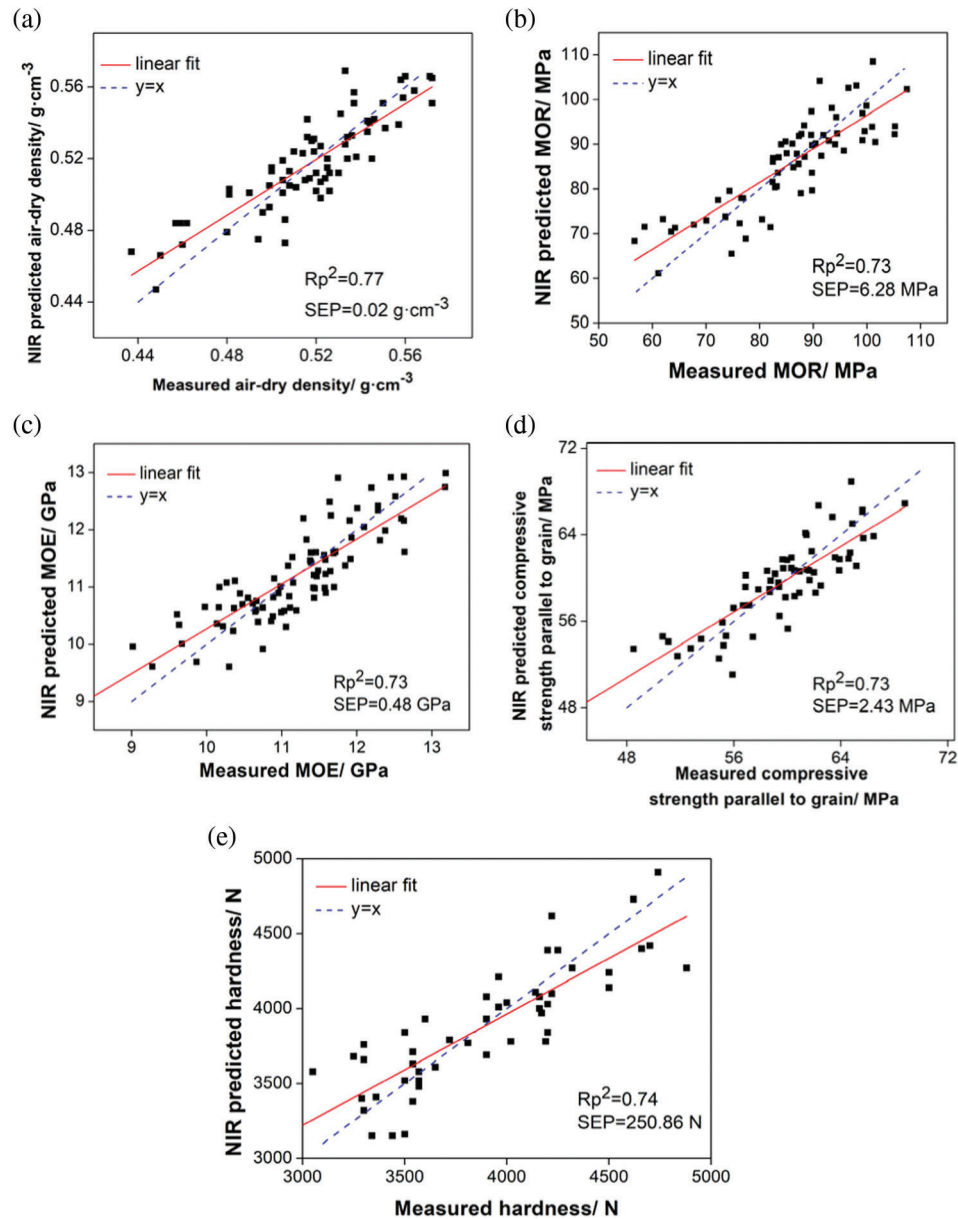| Pretreatment methods	Rc^2	SEC	Rp^2	SEP	Bias	RPD
1stDer + S-G	0.827	0.011	0.389	0.022	1.32×10^{-4}	1.28
2ndDer + S-G	0.847	0.011	0.133	0.028	4.93×10^{-4}	1.07
MSC + S-G	0.861	0.011	0.765	0.015	6.91×10^{-9}	2.07

Figure 5: The relationship between the measured value and NIR predicted value for physical and mechanical properties: air-dry density (a); MOR (b); MOE (c); compressive strength parallel to grain (d); hardness (e)

3.6 NIR Model Development of Mechanical Properties

3.6.1 PLS Model of MOR

Table 6 showed the relevant parameters of the MOR calibration models and prediction models established by using different section spectra and different pretreatment methods. The results based on the average spectra of two sections were considered best for MOR because of higher Rp^2 and RPD values. Therefore, it would better to use the average spectra of the two sections to establish the MOR model, which can be explained as the average spectra of the radial section and the tangential section contained more information.

Table 6: Summary of the NIR results for MOR based on different section spectra and pretreatment methods

Spectra sources	Evaluation indexes	Pretreatment methods		
		1stDer + S-G	2ndDer + S-G	MSC+ S-G
Radial section	Rc^2	0.608	0.745	0.785
	SEC	6.29	4.22	5.00
	Rp^2	0.491	0.507	0.676
	SEP	7.25	5.95	6.20
	Bias	0.418	−0.0962	0.0417
	RPD	1.39	1.41	1.75
Tangential section	Rc^2	0.725	0.666	0.808
	SEC	5.23	4.74	4.46
	Rp^2	0.504	0.488	0.599
	SEP	7.10	5.95	6.21
	Bias	−0.133	0.0698	−0.134
	RPD	1.41	1.39	1.57
Average sections	Rc^2	0.766	0.799	0.785
	SEC	4.66	3.93	5.52
	Rp^2	0.610	0.627	0.730
	SEP	6.09	5.42	6.28
	Bias	−0.0196	0.150	0.0491
	RPD	1.59	1.63	1.91

By analyzing the influence of different pretreatment methods on the prediction model results, MSC + S-G was the most applicable pretreatment method. When using the MSC + S-G pretreatment method, the Rp^2 values ranged from 0.676 to 0.730, and the RPD value was between 1.57 and 1.91. RPD value of about 1.5 was considered satisfactory for initial screening in tree breeding programs especially [44,45]. Fig. 5b showed a significant relationship between the predicted values and actual values of MOR for 3 *C. bungei* clones.

Considering the fast and convenient advantages of NIR, whether the modeling requirements can be met is worthy to be investigated while reducing the workload if only three points were taken in the spectra scanning. Table 7 showed the difference in modeling results between the three-point and five-point sampling methods. Overall, results based on five-point sampling methods were considered better than those from three-point sampling methods. More spectra points mean more collection information, which can better represent the nature of the entire sample. Compared with the five-point sampling method, the Rc^2 value of the model established with the three-point sampling method increased by 7.59%, while the Rp^2 value and RPD value decreased by 4.11% and 5.76%. It indicated that the three-point sampling method can be selected to reduce the workload of modeling and improve the efficiency of prediction under the condition that the prediction accuracy of the sample model was guaranteed.

Table 7: Summary of the NIR results for MOR and MOE based on different sampling points

Properties	Sampling points	Rc^2	SEC	Rp^2	SEP	Bias	RPD
MOR	3	0.849	4.15	0.696	5.97	0.0651	1.80
	5	0.785	5.52	0.730	6.28	0.0491	1.91
MOE	3	0.799	0.403	0.664	0.527	0.008	1.72
	5	0.876	0.324	0.728	0.485	0.0145	1.91

3.6.2 PLS Model of MOE

Taking 3 *C. bungei* clones as the research object, the effects of spectra from different sections and pretreatment methods on the NIR calibration model and prediction model of MOE were explored (Table 8). It can be concluded that models established by using the average spectra of the two sections were slightly better than the radial section and tangential section. The most promising predictive models were obtained from average sections, with the Rc^2 value of 0.876, the Rp^2 value of 0.728, and the RPD value of 1.91.

Table 8: Summary of the NIR results for MOE based on different section spectra and pretreatment methods

Spectra sources	Evaluation indexes	Pretreatment methods		
		1stDer + S-G	2ndDer + S-G	MSC + S-G
Radial section	Rc^2	0.752	0.816	0.821
	SEC	0.469	0.380	0.441
	Rp^2	0.635	0.636	0.724
	SEP	0.574	0.539	0.554
	Bias	9.39×10^{-3}	1.21×10^{-3}	6.84×10^{-3}
	RPD	1.65	1.65	1.89
Tangential section	Rc^2	0.784	0.831	0.709
	SEC	0.419	0.378	0.497
	Rp^2	0.619	0.696	0.633
	SEP	0.562	0.516	0.564
	Bias	2.60×10^{-3}	4.83×10^{-3}	-3.92×10^{-3}
	RPD	1.61	1.80	1.64
Average sections	Rc^2	0.807	0.856	0.876
	SEC	0.401	0.334	0.324
	Rp^2	0.650	0.715	0.728
	SEP	0.547	0.475	0.485
	Bias	0.0136	−0.0105	0.0145
	RPD	1.68	1.86	1.91

When comparing different pretreatment methods, it can be shown that the 2ndDer + S-G smoothing method was more applicable for the tangential section. The MSC + S-G smoothing method was used to preprocess the average spectra, and the prediction model established after preprocessing was the best. Fig. 5c showed a significant relationship between the predicted values and measured values of MOE for 3 *C. bungei* clones. NIR spectroscopy can be used as a preliminary detection tool to predict MOE capability since most models met the 1.5 RPD standard [45].

Table 7 listed the NIR models of the MOE of *C. bungei* clones based on different sampling points. The Rc^2, Rp^2, and RPD value of the model established by using three-point sampling method are reduced by about 9.09%, 9.59%, and 9.47%, respectively, compared with five-point sampling method. The accuracy of the model established by using the five-point sampling method was slightly higher than that by using the three-point sampling method. The data showed that the three-point sampling method can be used to reduce the experimental amount under the guarantee of certain modeling accuracy, so the three-point sampling method can be used for rapid NIR prediction of the MOE.

3.6.3 PLS Model of Compressive Strength Parallel to Grain

The effects of different pretreatment methods and spectra sources on the effect of compressive strength parallel to grain NIR model were investigated (Table 9). By comparing the spectral information of different sections, the Rc^2 and Rp^2 of cross section models were the highest, followed by the radial section and the tangential section. This was related to the fact that the cross section contained the most valid information.

Table 9: Summary of the NIR results for compressive strength parallel to grain based on different section spectra and pretreatment methods

Spectra sources	Evaluation indexes	Pretreatment methods		
		1stDer + S-G	2ndDer + S-G	MSC + S-G
Cross section	Rc^2	0.511	0.704	0.901
	SEC	2.81	2.14	1.45
	Rp^2	0.408	0.427	0.731
	SEP	3.14	3.02	2.43
	Bias	0.0122	-3.34×10^{-3}	0.0106
	RPD	1.29	1.34	1.91
Radial section	Rc^2	0.530	0.565	0.770
	SEC	3.59	3.39	2.45
	Rp^2	0.432	0.439	0.641
	SEP	4.00	3.91	3.11
	Bias	0.0130	−0.0137	0.0129
	RPD	1.32	1.32	1.66
Tangential section	Rc^2	0.850	0.566	0.739
	SEC	1.92	3.87	2.56
	Rp^2	0.634	0.447	0.668
	SEP	3.04	4.48	2.92
	Bias	0.0395	0.0446	−0.0539
	RPD	1.64	1.32	1.73

(Continued)

3298   JRM, 2022, vol.10, no.12

Table 9 (continued)

Spectra sources	Evaluation indexes	Pretreatment methods		
		1stDer + S-G	2ndDer + S-G	MSC + S-G
Average sections	Rc^2	0.487	0.519	0.813
	SEC	4.02	3.84	2.46
	Rp^2	0.341	0.376	0.655
	SEP	4.63	4.48	3.39
	Bias	0.0276	0.0446	2.51×10^{-3}
	RPD	1.22	1.26	1.69

Analysis demonstrated that MSC + S-G was the most effective pretreatment method to improve the model accuracy no matter in cross section, radial section, tangential section, or average sections. The 1stDer + S-G and 2ndDer + S-G smoothing methods were not effective enough to predict the compressive strength parallel to grain. For the model based on the spectra obtained from cross section prepossessed by MSC + S-G, the Rp^2 value was 0.731, the Rc^2 value was 0.901 and the RPD value was 1.91. It can be observed that the measured values had a high correlation with the predicted values of NIR spectra (Fig. 5d). To sum up, for the establishment of NIR model for the compressive strength parallel to grain of *C. bungei* clones, the model obtained by using the cross section spectral information and MSC + S-G method was the best. The results showed that NIR spectra and PLS regression model could be used to predict the compressive performance.

3.6.4 PLS Model of Hardness

Using the NIR spectroscopy information of the cross section, radial section, tangential section and average sections of the hardness samples of 3 *C. bungei* clones combined with 3 differed pretreatment methods to establish the hardness PLS models. According to Table 10, among the three sections, when the NIR calibration model was established by using the spectral from the cross section, the Rc^2 value was the highest, which was between 0.915–0.948.

Table 10: Summary of the NIR results for hardness based on different section spectra and pretreatment methods

Spectra sources	Evaluation indexes	Pretreatment methods		
		1stDer + S-G	2ndDer + S-G	MSC + S-G
Cross section	Rc^2	0.918	0.915	0.948
	SEC	150	153	109
	Rp^2	0.579	0.553	0.738
	SEP	348	359	251
	Bias	−8.92	−5.79	−4.01
	RPD	1.52	1.48	1.93
Radial section	Rc^2	0.451	0.428	0.644
	SEC	246	251	221
	Rp^2	0.300	0.280	0.601
	SEP	284	288	239
	Bias	−3.04	−5.31	2.79
	RPD	1.18	1.17	1.57

(Continued)

Table 10 (continued)

Spectra sources	Evaluation indexes	Pretreatment methods		
		1stDer + S-G	2ndDer + S-G	MSC + S-G
Tangential section	Rc^2	0.692	0.752	0.789
	SEC	261	218	211
	Rp^2	0.546	0.525	0.683
	SEP	323	307	214
	Bias	4.13	−9.47	12.7
	RPD	1.47	1.44	1.76
Average sections	Rc^2	0.545	0.601	0.74
	SEC	349	302	250
	Rp^2	0.365	0.382	0.623
	SEP	423	385	307
	Bias	3.18	−8.23	−11.1
	RPD	1.24	1.26	1.61

Comparing with different pretreatment methods, it was found that MSC + S-G smoothing method was used to obtain a better model effect, and the 1stDer + S-G smoothing method was superior to the 2ndDer + S-G pretreatment method. Based on the information above, the NIR prediction model of *C. bungei* wood hardness established by spectra collected on cross section preprocessed by the MSC + S-G method had the best effect, with the Rp^2 value of 0.738 and RPD value of 1.93. Strong correlation has been found between data measured experimentally and NIR-predicted data for hardness (Fig. 5e). Modeling data showed that NIR spectroscopy technology can complete the prediction of the hardness of *C. bungei* wood.

At present, NIR spectroscopy has not been used to predict the physical and mechanical properties of *C. bungei* wood. In this study, the NIR-based PLS models for predicting air-dry density, MOR, MOE, compressive strength parallel to grain, and hardness were established. The Rp^2 were above 0.7, while exceeding 0.76 for some of the NIR models. The results showed that NIR spectroscopy could be used to estimate the physical and mechanical properties of *C. bungei* wood quickly and reliably. Compressive strength parallel to grain and harness models constructed with spectra collected from cross section had better accuracy due to higher absorbance of cross section. The bending performance model based on the average spectra of radial and tangential sections was the best. This conclusion was in line with previous literature on wood, such as *Eucalyptus pellita* [46]. Among the 3 pretreatment methods, MSC + S-G was the best pretreatment method for the establishment of physical and mechanical properties. Compared with five-point sampling methods, the model using the three-point sampling method was less effective, but it can also complete the preliminary prediction. Regarding physical and mechanical properties, most of RPD were $1.5 < RPD < 2$, indicating that more applicable modeling methods should be further developed to improve the accuracy of the NIR model of *C. bungei*.

4 Conclusions

The air-dry density and main mechanical properties of those three *C. bungei* clones, 'Luoqiu 2', 'Luoqiu 3', and 'Luoqiu 5' have been evaluated in this study, in which 'Luoqiu 3' exhibited biggest potential for further application. The physical and mechanical properties of outerwood samples were

higher than those of corewood samples. There were extremely significant positive correlations between the air-dry density and various mechanical properties of wood at the level of $P < 0.01$. Air-dry density, compressive strength parallel to grain, and hardness models established with spectra of the cross section had better effects, while the average spectra of radial section and tangential section was more suitable for modeling the bending performance. The results showed that PLS based on NIR spectra pretreated by MSC + S-G smoothing method to evaluate air-dry density and mechanical properties of *C. bungei* clones were promising. On the premise of ensuring the accuracy of the model, the three-point sampling methods can be used to collect the NIR spectra of bending performance. This study demonstrated that NIR spectroscopy can be used as a high throughput method to non-destructively estimate important wood traits for rare *C. bungei* clones. And the accuracy and robustness of the prediction model of physical and mechanical properties of *C. bungei* wood can be improved by increasing the sample numbers with bigger coefficient of variation and adopting dimension reduction analysis of NIR spectral data in the subsequent model optimization study.

Conflicts of Interest: The authors declare that they have no conflicts of interest to report regarding the present study.

References

1. Deng, L., Ren, S., Lv, J., Wang, Y., Ren, H. et al. (2019). Grow characteristics and variation of heartwood and sapwood of *Catalpa bungei. China Wood Industry, 33(4),* 9–13. DOI 10.19455/j.mcgy.20190403.

2. Teranishi, M., Koizumi, A., Hirai, T. (2008). Evaluation of quality indexes of bending performance and hardness for hardwoods. *Journal of Wood Science, 54(5),* 423–428. DOI 10.1007/s10086-008-0969-1.

3. Hamid, N. H. A., Ahmad, M., Suratman, M. N. (2013). Bending and compression properties of Malaysian medium hardwood in orthotropic directions Kelat (*Syzygium* spp.). *Applied Mechanics and Materials, 330,* 938–941. DOI 10.4028/www.scientific.net/AMM.330.938.

4. Ayanleye, S., Avramidis, S. (2020). Predictive capacity of some wood properties by near-infrared spectroscopy. *International Wood Products Journal, 12(2),* 83–94. DOI 10.1080/20426445.2020.1834312.

5. Liang, H., Xing, L., Wen, J., Gao, C., Lin, J. (2020). Near-infrared spectroscopy detection method for compressive strength of *Fraxinus mandschurica. International Journal of Circuits, Systems and Signal Processing, 14,* 108–113. DOI 10.46300/9106.2020.14.17.

6. Diaconu, D., Wassenberg, M., Spiecker, H. (2016). Variability of European beech wood density as influenced by interactions between tree ring growth and aspect. *Forest Ecosystems, 3,* 165–173. DOI 10.1186/s40663-016-0065-8.

7. Won, K., Kim, T. K., Hwang, K., Chong, S., Byeon, H. (2012). Effect of heat treatment on the bending strength and hardness of wood. *Journal of the Korean Wood Science & Technology, 40(5),* 303–310. DOI 10.5658/WOOD.2012.40.5.303.

8. Liu, S., Zhang, J., Zhihua, H., Duan, F., Liu, Y. (2008). Physical and mechanical properties of *Catalap bungei* (Wanqing number 1). *Journal of Anhui Agricultural University, 35(4),* 473–477. DOI 10.13610/j.cnki.1672-352x.2008.04.019.

9. Ma, W., Zhang, S., Wang, J., Zhai, W., Cui, Y. et al. (2013). Timber physical and mechanical properties of new *Catalpa bungei* clones. *Scientia Silvae Sinicae, 49(9),* 126–134. DOI 10.11707/j.1001-7488.20130918.

10. Tsuchikawa, S., Kobori, H. (2015). A review of recent application of near infrared spectroscopy to wood science and technology. *Journal of Wood Science, 61(3),* 213–220. DOI 10.1007/s10086-015-1467-x.

11. Schimleck, L. R., Mora, C., Daniels, R. F. (2003). Estimation of the physical wood properties of green *Pinus taeda* radial samples by near infrared spectroscopy. *Canadian Journal of Forest Research, 33(12),* 2297–2305. DOI 10.1139/x03-173.

12. Adedipe, O. E., Dawson-Andoh, B. (2008). Prediction of yellow-poplar (*Liriodendron tulipifera*) veneer stiffness and bulk density using near infrared spectroscopy and multivariate calibration. *Journal of Near Infrared Spectroscopy, 16(5),* 487–496. DOI 10.1255/jnirs.812.

13. Raturi, A., Kothiyal, V., Uniyal, K. K., Semalty, P. D. (2012). Development and evaluation of models for specific gravity of *Eucalyptus tereticornis* wood by Fourier transformed near infrared spectroscopy and partial least squares regression analysis. *Journal of the Indian Academy of Wood Science, 9(1),* 40–45. DOI 10.1007/s13196-012-0069-0.

14. Yu, L., Liang, Y., Zhang, Y., Cao, J. (2019). Mechanical properties of wood materials using near-infrared spectroscopy based on correlation local embedding and partial least-squares. *Journal of Forestry Research, 31(3),* 1053–1060. DOI 10.1007/s11676-019-01031-7.

15. Schimleck, L., Matos, J. L., Oliveira, J. T., Muniz, G. (2011). Non-destructive estimation of pernambuco (*Caesalpinia echinata*) clear wood properties using near infrared spectroscopy. *Journal of Near Infrared Spectroscopy, 19,* 411. DOI 10.1255/jnirs.953.

16. Dahlen, J., Diaz, I., Schimleck, L., Jones, P. D. (2017). Near-infrared spectroscopy prediction of southern pine No. 2 lumber physical and mechanical properties. *Wood Science and Technology, 51(2),* 309–322. DOI 10.1007/s00226-016-0874-5.

17. Jia, R., Wang, Y., Wang, R., Chen, X. (2021). Physical and mechanical properties of poplar clones and rapid prediction of the properties by near infrared spectroscopy. *Forests, 12(2),* 206. DOI 10.3390/F12020206.

18. Schimleck, L. R., Jones, P. D., Clark, A., Daniels, R. F., Peter, G. F. (2005). Near infrared spectroscopy for the nondestructive estimation of clear wood properties of *Pinus taeda* L. from the southern United States. *Forest Products Journal, 55(12),* 21–28. DOI 10.1007/s10570-005-9010-7.

19. Schimleck, L., Matos, J. L. M., Trianoski, R., Prata, J. G. (2018). Comparison of methods for estimating mechanical properties of wood by NIR spectroscopy. *Journal of Spectroscopy, 2018,* 1–10. DOI 10.1155/2018/4823285.

20. Thumm, A., Meder, R. (2001). Stiffness prediction of *Radiata pine* clearwood test pieces using near infrared spectroscopy. *Journal of Near Infrared Spectroscopy, 9(2),* 117–122. DOI 10.1255/jnirs.298.

21. Zhao, N. (2016). *Research on the quantitative modeling method and robustness of traditional chinese medicine nir based on system science (Master Thesis).* Beijing University of Chinese Medicine, Beijing.

22. Wang, D., Ji, J., Gao, H. (2014). The effect of MSC spectral pretreatment regions on near infrared spectroscopy calibration results. *Spectroscopy and Spectra Analysis, 34(9),* 2387–2390. DOI 10.3964/j.issn.1000-0593(2014)09-2387-04.

23. Tong, Li., Zhang, W. (2016). Using Fourier transform near-infrared spectroscopy to predict the mechanical properties of thermally modified Southern pine wood. *Applied Spectroscopy, 70(10),* 1676–1684. DOI 10.1177/0003702816644453.

24. State Forestry Administration of the People's Republic of China (2009). Method for determination of the density of wood. Standard GB/T 1933-2009. Standards Press of China, Beijing, China.

25. State Forestry Administration of the People's Republic of China (2009). Method of determination of the modulus of elasticity in static bending of wood. Standard GB/T 1936.2-2009. Standards Press of China, Beijing, China.

26. State Forestry Administration of the People's Republic of China (2009). Method of testing in bending strength of wood. Standard GB/T (1936.1-2009). Standards Press of China, Beijing, China.

27. State Forestry Administration of the People's Republic of China (2009). Method of testing in compressive strength parallel to grain of wood. Standard GB/T 1935-2009. Standards Press of China, Beijing, China.

28. State Forestry Administration of the People's Republic of China (2009). Method of testing in hardness of wood. Standard GB/T 1941-2009. Standards Press of China, Beijing, China.

29. Xie, L., Ye, X., Liu, D., Ying, Y. (2009). Quantification of glucose, fructose and sucrose in bayberry juice by NIR and PLS. *Food Chemistry, 114(3),* 1135–1140. DOI 10.1016/j.foodchem.2008.10.076.

30. Ren, H., Zhong, X. (2006). Intratree variability of wood density and main wood mechanical properties in Chinese fir and poplar plantation. *Scientia Silvae Sinicae, 42(3),* 13–20. DOI 10.3321/j.issn:1001-7488.2006.03.003.

31. Yin, S. (1996). *Wood science*. Beijing: China Forestry Publishing House.

32. Li, W. (2013). *Catalpa bungei C.A.Mey clonal breeding (Master Thesis)*. Shandong Agricultural University, Shandong.

33. Mao, W., Xu, W., Huang, Q., Tang, X., Wu, Z. (2015). Building of wood selecting index for solid wood furniture based on mechanical property analysis. *Journal of Forestry Engineering, 29(6),* 127–131. DOI 10.13360/j.issn.1000-8101.2015.06.032.

34. Wu, W. (2015). *Study on the variance of wood structure and properties of Catalpa bungei C.A.Mey (Master Thesis)*. Nanjing Forestry University, Jiangsu.

35. Merela, M., Cufar, K. (2014). Density and mechanical properties of oak sapwood versus heartwood. *Drvna Industrija, 64,* 323–334. DOI 10.5552/drind.2013.1325.

36. Lu, G., Lin, Y., Kang, H. (2011). Wood properties variation in radial direction within trees of different aged *Acacia melanoxylon*. *Guangdong Forestry Science and Technology, 27(4),* 37–40.

37. Sun, h., Ji, X., Zhao, H., Yang, M., Cing, X. (2018). Physical and mechanical properties of *Robinia pseudoacacia* wood in artificial forests. *Journal of Beijing Forestry University, 40(7),* 104–112. DOI 10.13332/j.1000-1522.20180030.

38. Lv, Y., liu, Y., Fang, S., Tian, Y., Xi, X. (2018). Genetic variation in growth and wood properties for southern type poplar clones. *Journal of Nanjing Forestry University (Natural Sciences Edition), 42(6),* 20–26. DOI 10.3969/j.issn.1000-2006.201804024.

39. Workman, J. (2008). NIR spectroscopy calibration basics. In: D. A. Burns, E. W. Ciurczak (Eds.) *Handbook of near-infrared analysis*, pp. 123–130. Boca Raton: CRC Press.

40. Schimleck, L. R., Evans, R., Ilic, J. (2001). Estimation of *Eucalyptus delegatensis* wood properties by near infrared spectroscopy. *Canadian Journal of Forest Research, 31(10),* 1671–1675. DOI 10.1139/cjfr-31-10-1671.

41. Zhao, R., Huo, X., Shangguan, W., Wang, Y. (2011). Influence factor for prediction of air-dry density of *Eucalyptus pellita* by near infrared spectroscopy. *Spectroscopy and Spectra Analysis, 31(11),* 2948–2951. DOI 10.3964/j.issn.1000-0593(2011)11-2948-04.

42. Delwiche, S. R., Reeves, J. B. (2004). The effect of spectral pre-treatments on the partial least squares modelling of agricultural products. *Journal of Near Infrared Spectroscopy, 12(3),* 177–182. DOI 10.1255/jnirs.424.

43. Hein, P. R. G., Campos, A. C. M., Mendes, R. F., Mendes, L. M., Chaix, G. (2011). Estimation of physical and mechanical properties of agro-based particleboards by near infrared spectroscopy. *European Journal of Wood and Wood Products, 69(3),* 431–442. DOI 10.1007/s00107-010-0471-5.

44. Schimleck, L., Doran, J., Rimbawanto, A. (2003). Near infrared spectroscopy for cost effective screening of foliar oil characteristics in a *Melaleuca cajuputi* breeding population. *Journal of Agricultural and Food Chemistry, 51,* 2433–2437. DOI 10.1139/x03-173.

45. Acquah, G. E., Essien, C., Via, B. K., Billor, N., Eckhardt, L. G. (2018). Estimating the basic density and mechanical properties of Elite loblolly pine families with near infrared spectroscopy. *Forest Science, 64(2),* 149–158. DOI 10.1093/forsci/fxx009.

46. Zhao, R., Huo, X., Zhang, L. (2009). Estimation of modulus of elasticity of *Eucalyptus pellita* wood by near infrared spectroscopy. *Spectroscopy and Spectral Analysis, 29(9),* 2392–2395. DOI 10.3964/j.issn.1000-0593(2009)09-2392-04.